PP&L Pennsylvania Power & Light Company
Two North Ninth Street • Allentown, PA 18101 • 215 / 770-5151

Norman W. Curtis
Vice President-Engineering & Construction-Nuclear
215 / 770-5381

MAY 26 1982

Mr. A. Schwencer, Chief
Licensing Branch No. 2
U.S. Nuclear Regulatory Commission
Washington, D.C. 20555

SUSQUEHANNA STEAM ELECTRIC STATION
CHUGGING LOAD DEFINITION
ER 100450 FILE 172-08 Docket Nos. 50-387
PLA-1097 50-388

Dear Mr. Schwencer:

Per our letter PLA-1063 dated April 20, 1982, PP&L committed to providing additional information to close-out Dr. Bienkowski's concern with our chugging load definition. The attached provides this information and will be formally submitted via the SSES Design Assessment Report scheduled for submittal on June 8, 1982.

Very truly yours,

N W Curtis

N. W. Curtis
Vice President-Engineering & Construction-Nuclear

PAF/mks

Attachment

cc: F. Eltawalia - NRC

B001
S
1/1

RESPONSE TO NRC CONCERNS REGARDING THE SSES

CHUGGING LOAD SPECIFICATION

This submittal responds to a request from the NRC staff (Reference 1) to document arguments demonstrating the adequacy of the SSES chugging load specification. Essentially all of the information contained in this document was presented at a meeting held in San Jose, California on April 8, 1982 between representatives of the Mark II Owners Group, SSES personnel and members of the NRC staff.

Reference 1 specifies two elements required to address the staff's concerns:

"1. Formally document the material which was used to conclude that the asymmetric chugging load specification is not a major contributor to the structural response. Although not specifically discussed during the meeting, the response should address the validity of the rationale over the entire frequency range of interest (0 to 50 Hz).

2. Extend the JAERI comparisons to 20 different sets of start times to be generated in the same manner as outlined in the generic methodology. For each set of start times evaluate the response of applying the chugging sources to the JAERI facility and develop an envelope of the minimum of the twenty trials. Comparison of that envelope to experimental data obtained from JAERI would then be provided. If frequency "poke through" exists, justification would be provided as to why the current specification is adequate."

The following provides the proposed DAR write-up for PP&L's response to Dr. Bienkowski's concern described above. We expect to formally submit the subject response on June 8, 1982.

TABLE OF CONTENTS

1.0 CONTRIBUTION OF THE ASYMMETRIC CHUGGING LOAD SPECIFICATION TO PLANT STRUCTURAL RESPONSE

1.1 COMMENTS ON THE ASYMMETRIC CHUGGING LOAD CASE

This section provides comments on the effect of vent start times on the asymmetric pool wall loads generated during chugging. As with symmetric loads, a unique vent start time set (STS) will produce a unique asymmetric pool response. However, analysis of the complete pool transfer function shows that the primary asymmetric pool response in terms of a net "overturning" moment is generated only by the first asymmetric mode in the frequency range between 15-100 Hz. No other asymmetric modes produce a net overturning moment.

Figure 1-1 shows a schematic of the first asymmetric mode in the SSES pool geometry. The mode shape for the pressure generated by a single vent is a cosine function, therefore, the "area of influence" for that vent is quite large. Due to the "large area of influence", considerable overlapping occurs between adjacent vents.

Further, for the first asymmetric mode, pressure variation in the radial direction is small. This means that vents located on a given radial ray but at different radii have roughly the same effective "moment arm".

Finally, in a multivent geometry where events are randomly desynchronized (such as in the SSES case), the asymmetric mode is not stationary in space. It rotates; hence there is no fixed axis in time about which the asymmetric mode produces a full amplitude "overturning moment".

Due to these considerations, the effect of a selected STS on the "overturning moment" is much less than that predicted by simple analyses where the "area of influence" is taken to be a small area under each vent and the moment arm as the orthogonal distance between the vent and a fixed axis in time. It is expected, therefore, that in reality, the effect of vent start times on the asymmetric pool responses will be no more severe than those for the symmetric response.

1.2 GENERIC POSITION ON WNP-2 SUBMITTAL

The Mark II utilities and their respective A/Es have reviewed Part A of the WNP-2 report (Reference 2) and compared it with their own containment analyses. All utilities have concluded that Mark II plants exhibit overall characteristics and trends similar to those identified in the report:

- o There is no evidence that the Mark II containments "rock" due to hydrodynamic loads.

- o In a concrete containment, the plant response to chugging loads decreases as one moves away from the wetwell in the primary containment. Once outside the primary containment, the response is significantly reduced.

When reviewing separate responses for the symmetric and asymmetric chugging load, very little difference is observed. This result has been confirmed on the WNP-2 plant with a subsequent submittal to the NRC. (Reference 3).

As an additional example of the structural response, this time for the SSES concrete containment, selected accelerating response spectra (ARS) curves generated with our chugging load definition are presented in Figures 1-3 through 1-10. Each figure compares the ARS curves for the symmetric and asymmetric at the node points in the ANSYS model identified in Figure 1-2. For most containment locations, the symmetric and asymmetric ARS curves are quite similar in both frequency content and amplitude. Also, observe the decrease in amplitude of the responses at increasing elevation above the containment basemat. The curves represent the envelop of all design sources.

However, in some containment locations, at certain frequencies the symmetric ARS curves exceed the asymmetric ARS curves, and vice versa, by more than 10%. Our explanation is as follows:

- o Figures 1-3 to 1-6: These figures show the responses in the vertical direction at elevations above the diaphragm slab. These figures indicate that the symmetric response always exceeds the asymmetric, and at some frequencies by more than 10%. This is expected, since the symmetric source distribution was specified to maximize the vertical pressures on the containment basemat. These pressures would excite the vertical modes of the containment in a more significant manner, than the asymmetric case. This is especially true in the low frequencies, where desynchronization does not significantly effect the pressure response, and the symmetric source distribution leads to a greater source strength than the asymmetric load case. This greater source strength in low frequencies, also excites the higher frequencies as explained in the JAERI PRS comparison (Subsection 2.3.2).

- Figure 1-7: Please note that the ARS curves for Node 841, direction X, presented at April 8, 1982 NRC/SSES meeting and documented in PLA-1063 were labeled incorrectly. The curves should be reversed, such that the asymmetric ARS curve now exceeds the symmetric curve in the low frequencies. Figure 1-7 shows the correct labeling of the curves.

  At all frequencies, except between 4 and 8 Hz, the two load cases compare quite well. As a result, we requested that Bechrel examine the natural frequencies and participation factors for Node 841. They indicated that in these low frequencies, there are significant modes in the horizontal direction. Thus, one would expect the asymmetric response to exceed the symmetric response for Node 841 at these frequencies, since desynchronization does not significantly effect the pressure distribution at these low frequencies and the asymmetric source distribution was specified to maximize the asymmetry in the containment.

- Figure 1-8: This figure exhibits a similar comparison as Figure 1-7. Again, at these low frequencies, Node 411 contains significant lateral modes. Thus, as for Figure 1-7, one would expect the asymmetric response to exceed the symmetric response.

- Figure 1-9: This figure indicates that above 30 Hz the symmetric response exceeds the asymmetric response by a large margin. At this containment azimuth location, we determined that the Mean Square Power (MSP) for the pressure at the intersection of the containment wall and basemat, varies for the symmetric and asymmetric load case. Our analysis indicated that the symmetric MSP exceeds the asymmetric MSP at this azimuth location; probably due to the effects of the chug start times for downcomers in close proximity to this azimuth angle. Because of this, one would expect the symmetric case to exceed the asymmetric case.

- Figure 1-10: For all frequencies, the symmetric and asymmetric load cases exhibit a similar response.

Thus, even with the source strength unbalance imposed by the asymmetric chugging load definition, the structural response is not noticeably different from that of the symmetric load case.

It can be concluded from the preceding discussion that the overturning moment associated with asymmetric chugging need not be used as a criterion in assessing the adequacy of the load definition. This is true for the reasons outlined in Subsection 1.1 and because the asymmetric pressure distribution can also be found in the symmetric load specification due to source desynchronization. Thus, the adequacy of the SSES chugging load definition can be demonstrated through a comparison of the symmetric load specification with the multivent JAERI data.

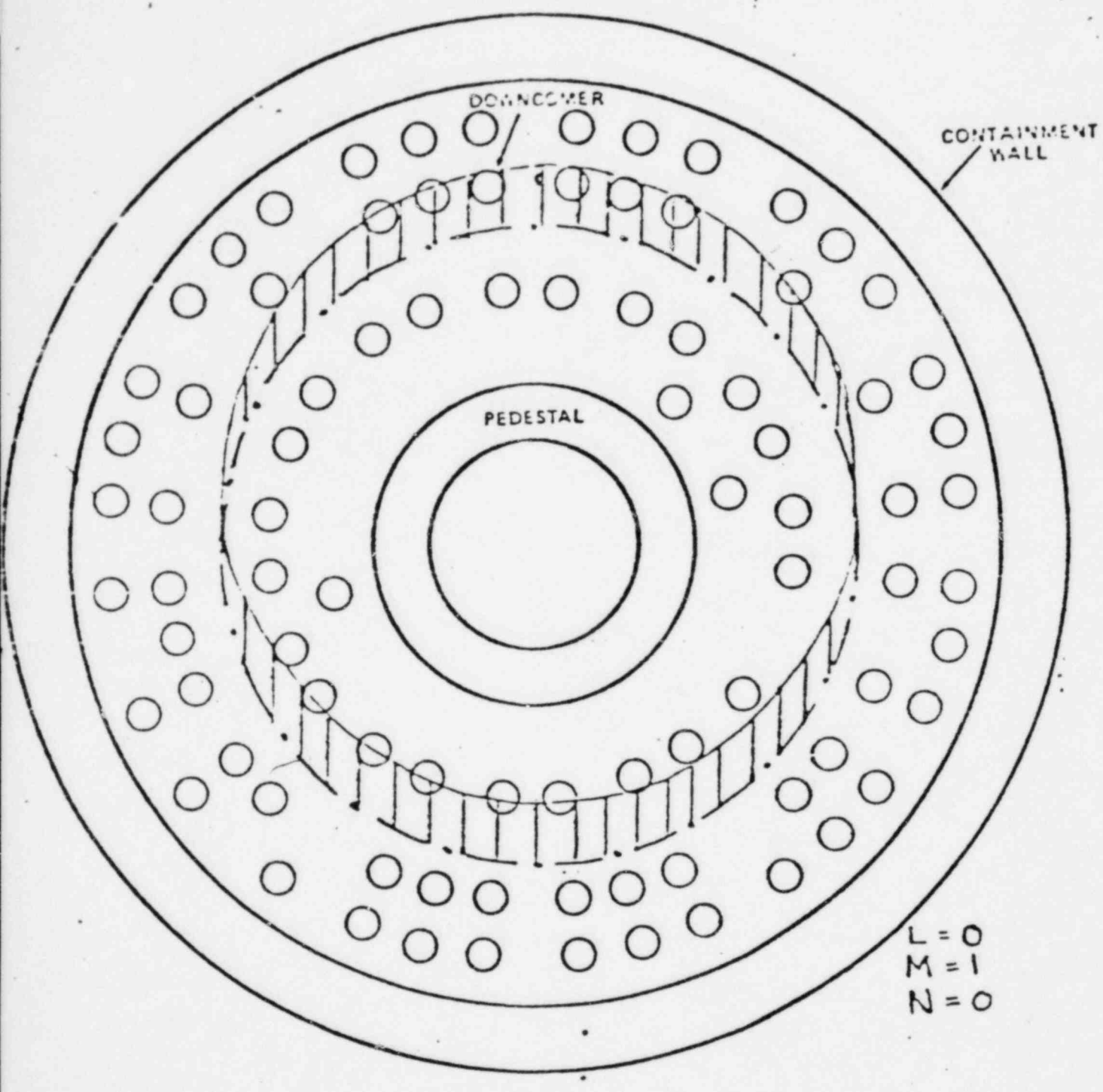

Figure 1-1. SCHEMATIC OF THE FIRST ASYMMETRIC POOL MODE

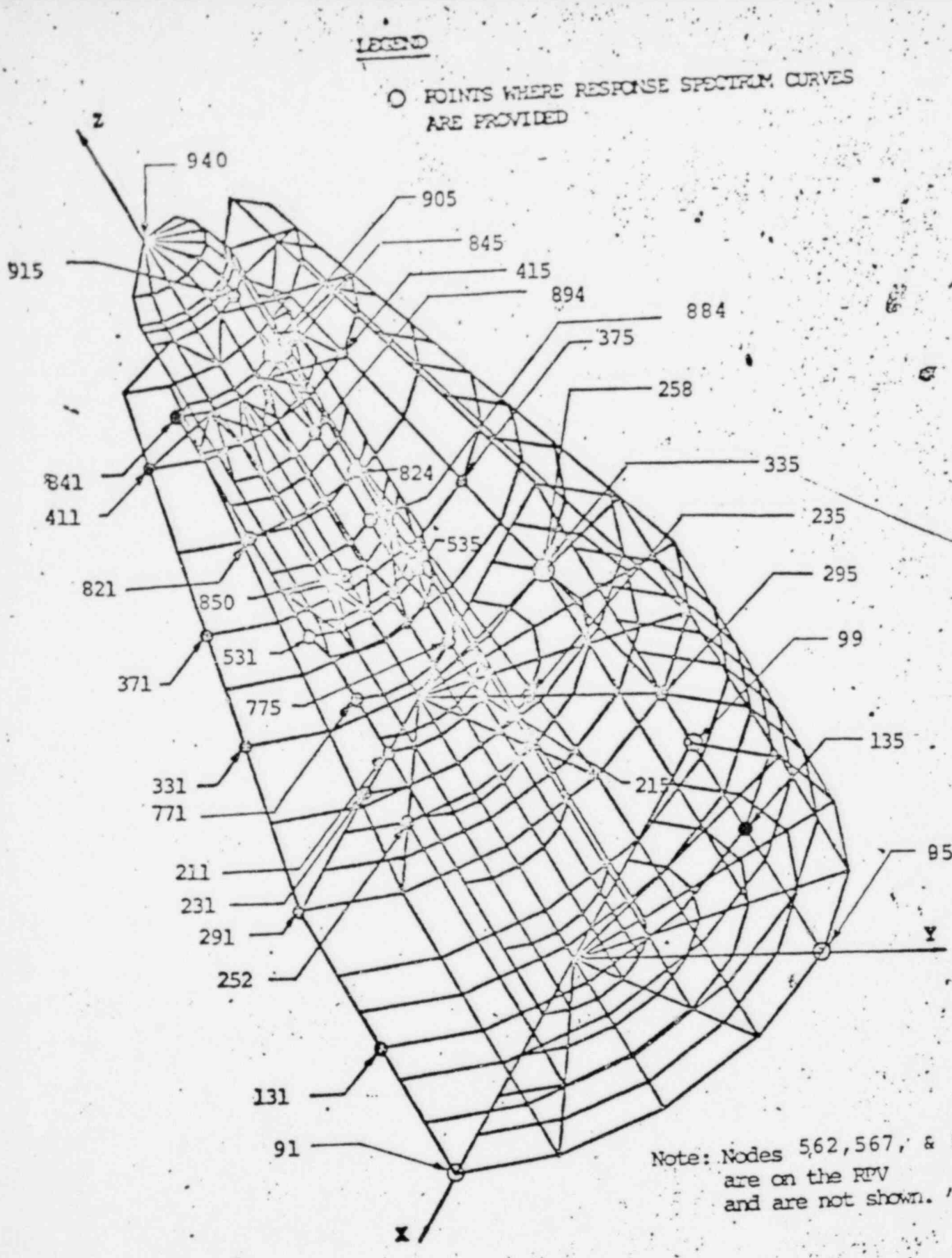
LEGEND
○ POINTS WHERE RESPONSE SPECTRUM CURVES ARE PROVIDED
Z
940
905
845
915
415
894
884
375
258
841
824
335
411
235
535
821
295
850
99
531
371
775
135
331
215
771
85
211
231
Y
291
252
131
91
X
Note: Nodes 562, 567, & 568 are on the RPV and are not shown.

Figure 1-2

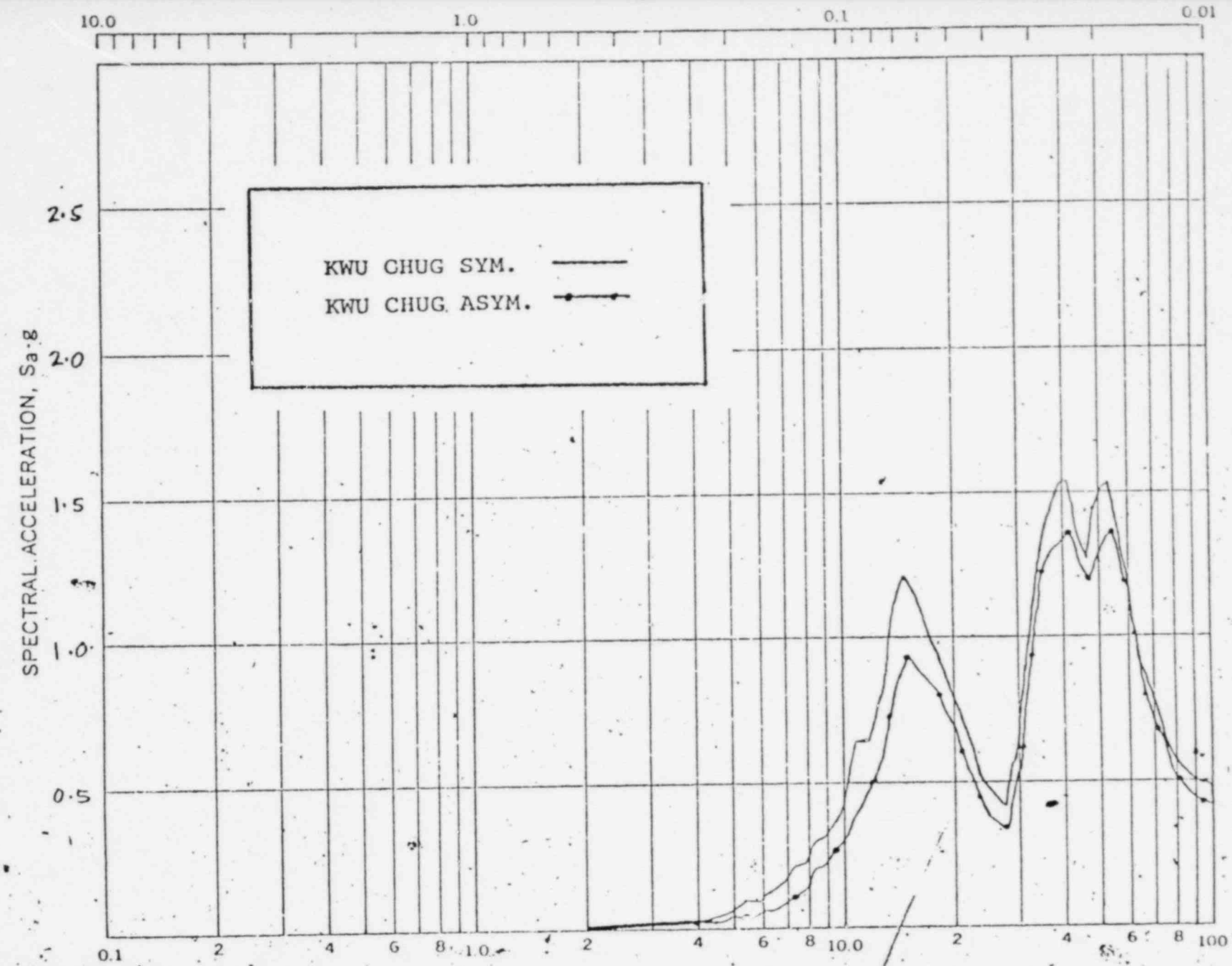

Acceleration Spectra for RPV SHIELD

Load Case: Susquehanna KWU CHUG SYM. VS ASYM.

Node 841, Direction Z, Elev 778' - 9-3/4"

Damping: 0.02

Figure I-3

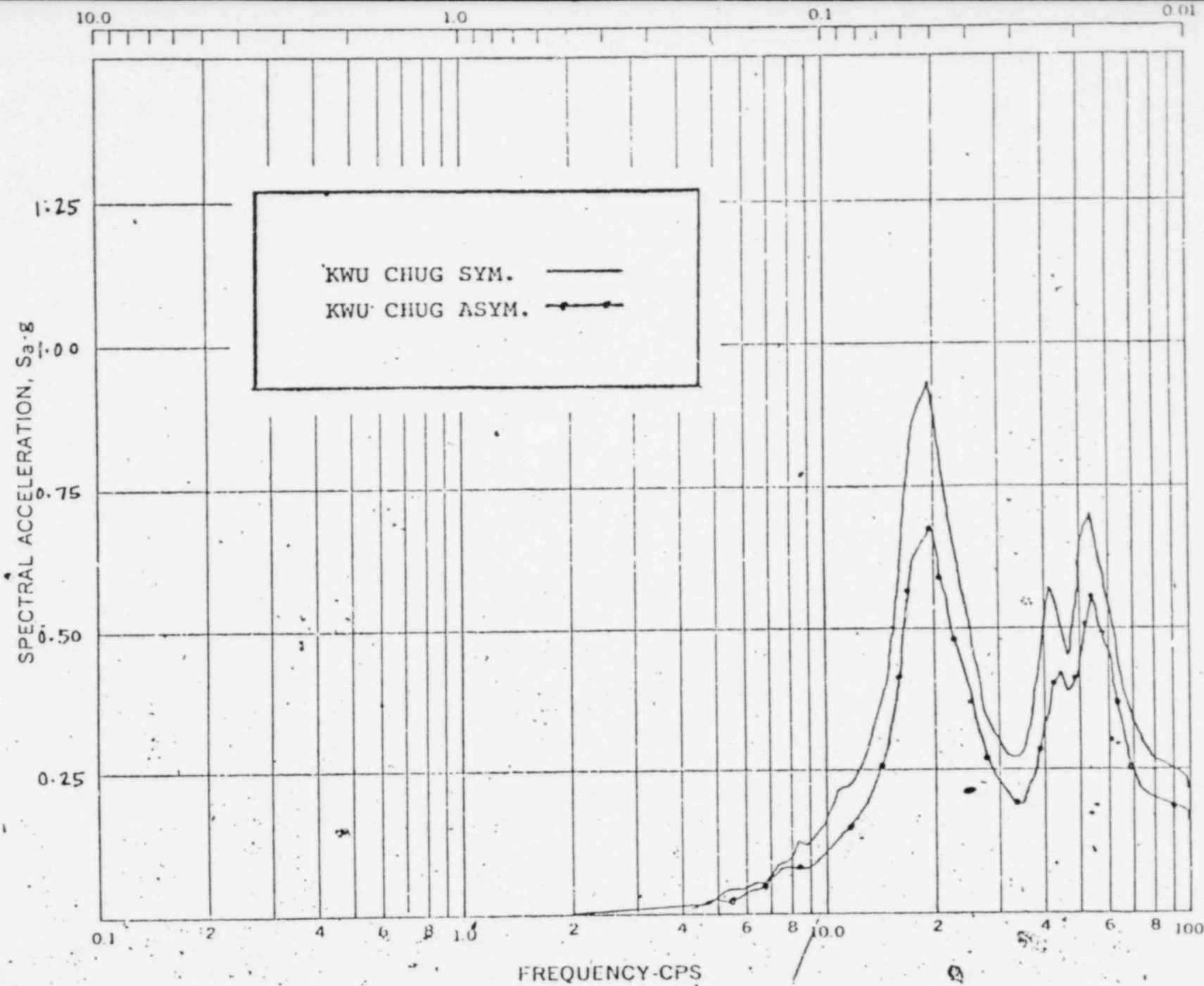

Acceleration Spectra for CONTAINMENT SHELL

Load Case: Susquehanna KWU CHUG SYM. VS ASYM.

Node 411, Direction Z, Elev 778' - 9-3/4"

Damping: 0.02

Figure 1-4

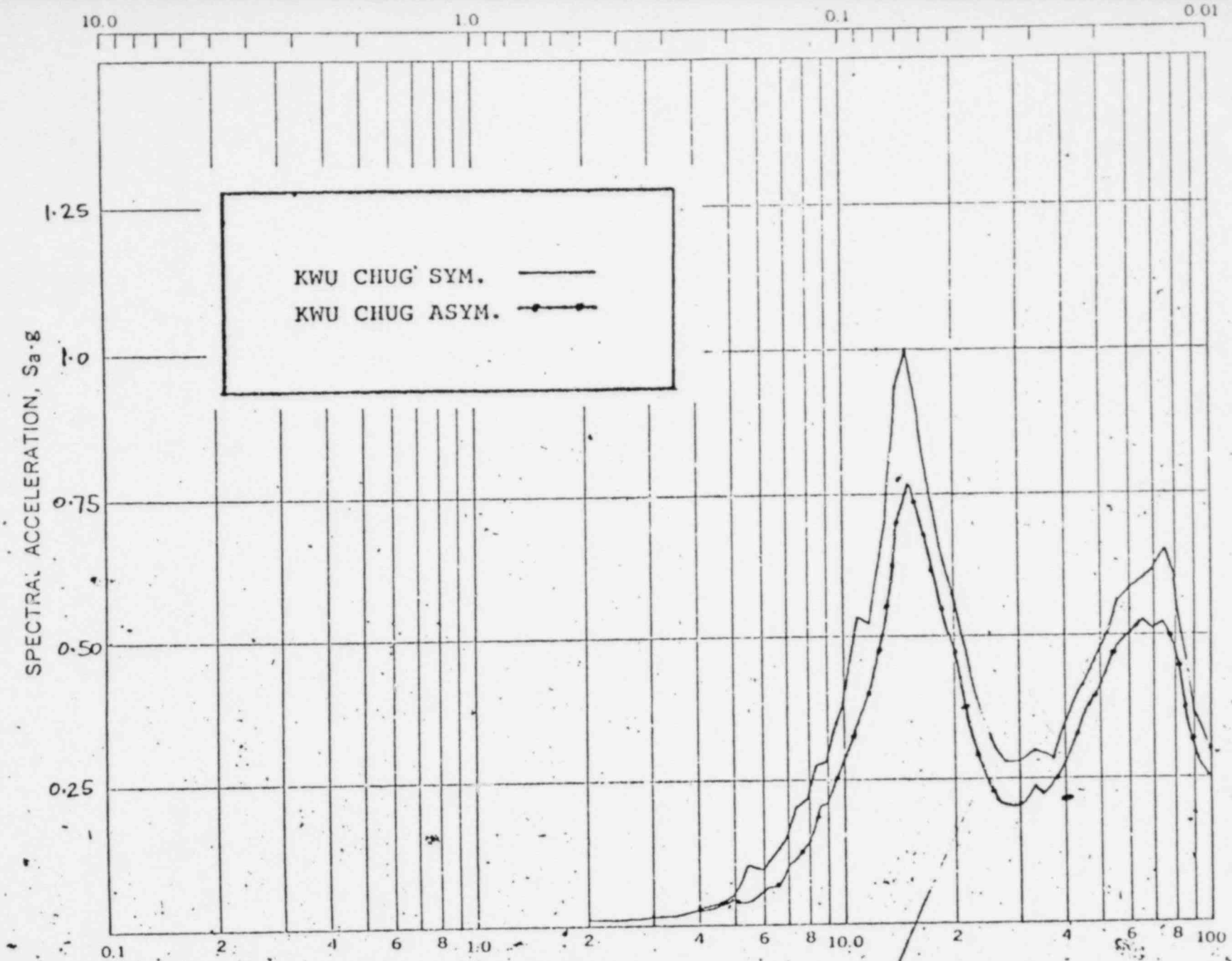

Acceleration Spectra for PEDESTAL

Load Case: Synychenng KWU CHUG SYM. VS ASYM.

Node 771, Direction Z, Elev 714' - 1-1/2"

Damping: 0.02

Figure 1-5

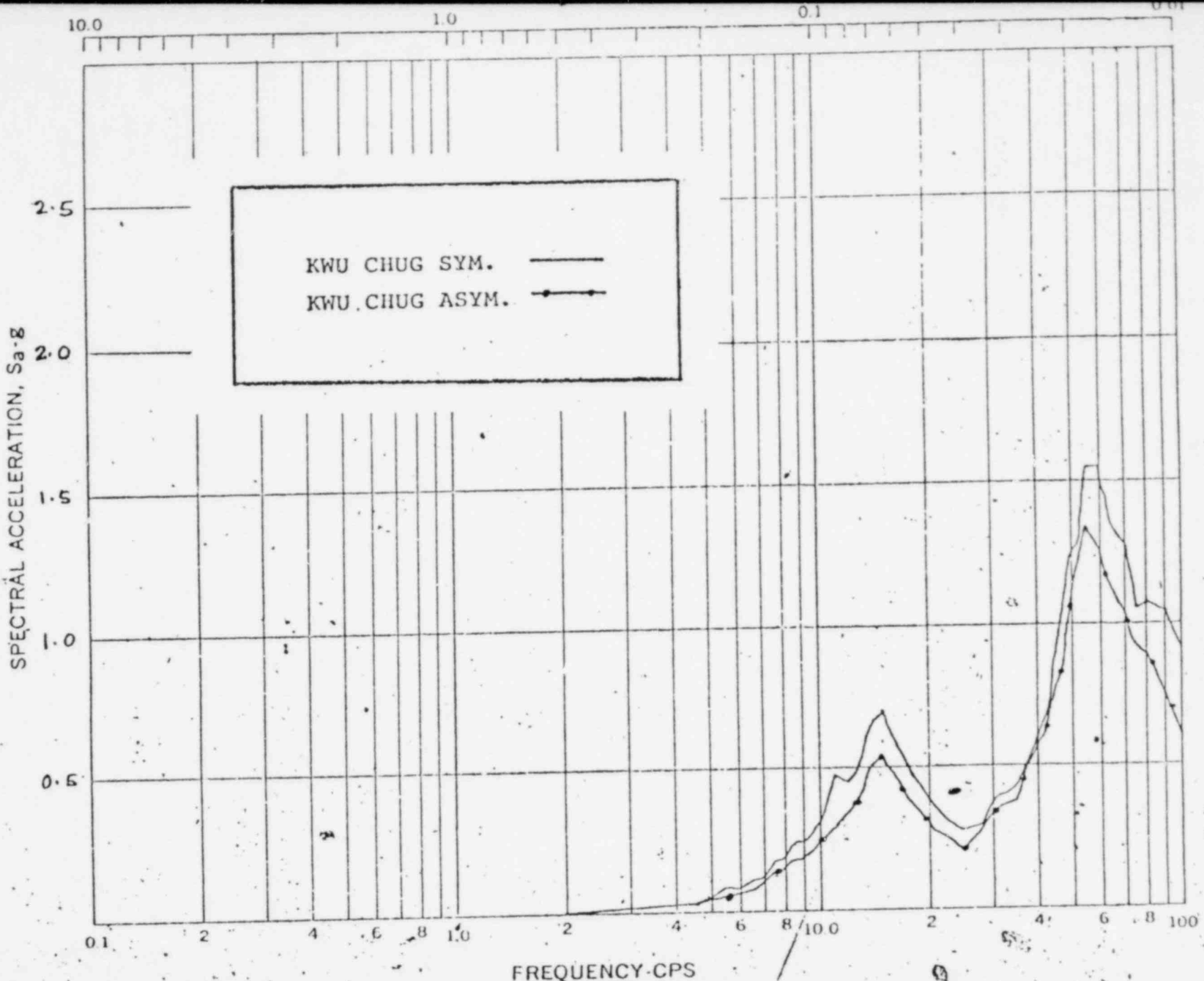

Acceleration Spectra for DIAPHRAGM SLAB

Load Case: Susquehanna KWU CHUG SYM. VS ASYM.

Node 235, Direction Z, Elev 702'-3"

Damping: 0.02

Figure 1-6

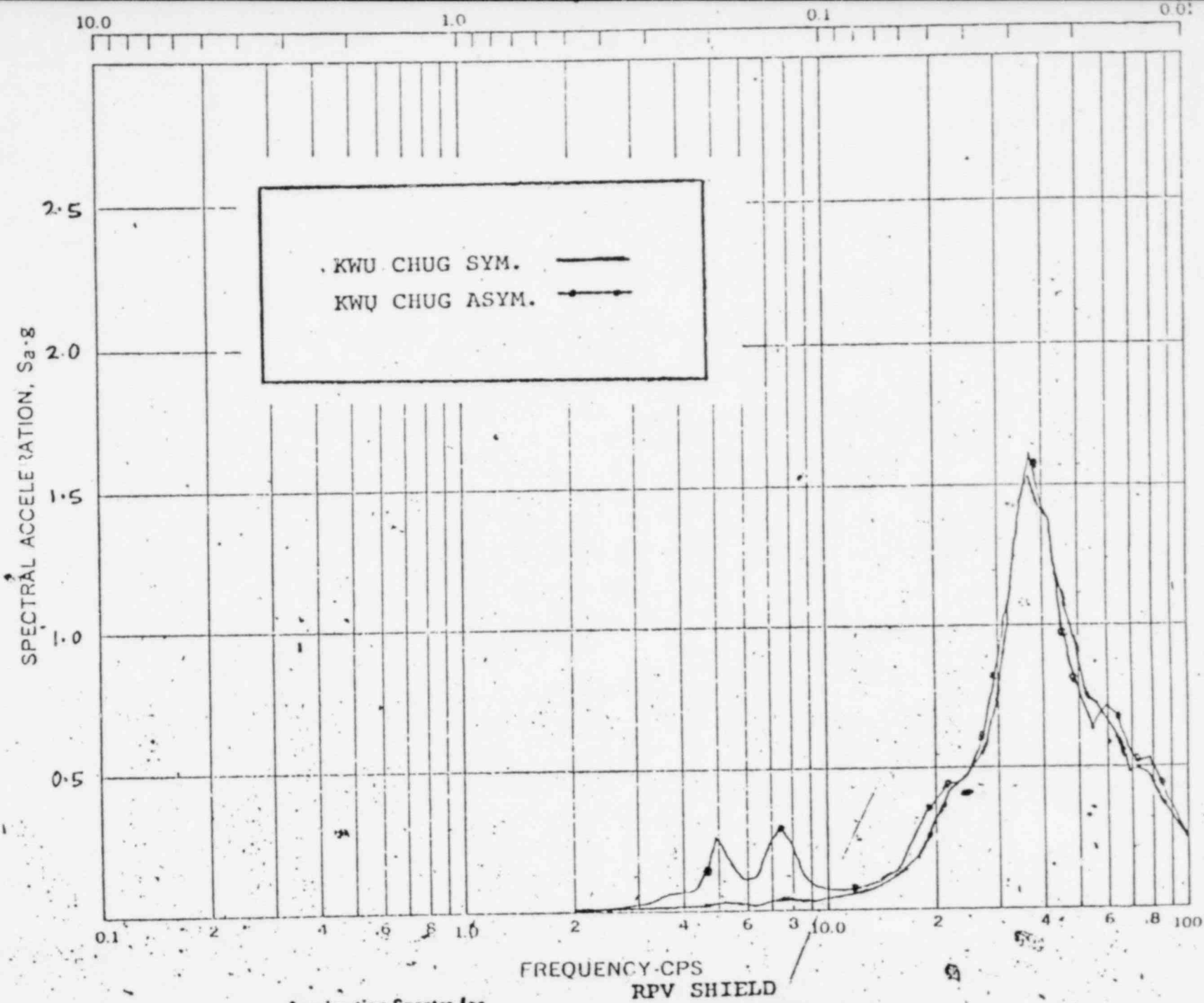

RPV SHIELD

Acceleration Spectra for _____

Load Case: Susquehanna KWU CHUG SYM. VS ASYM.

Node 841, Direction X, Elev 778' - 9-3/4"

Damping: 0.02

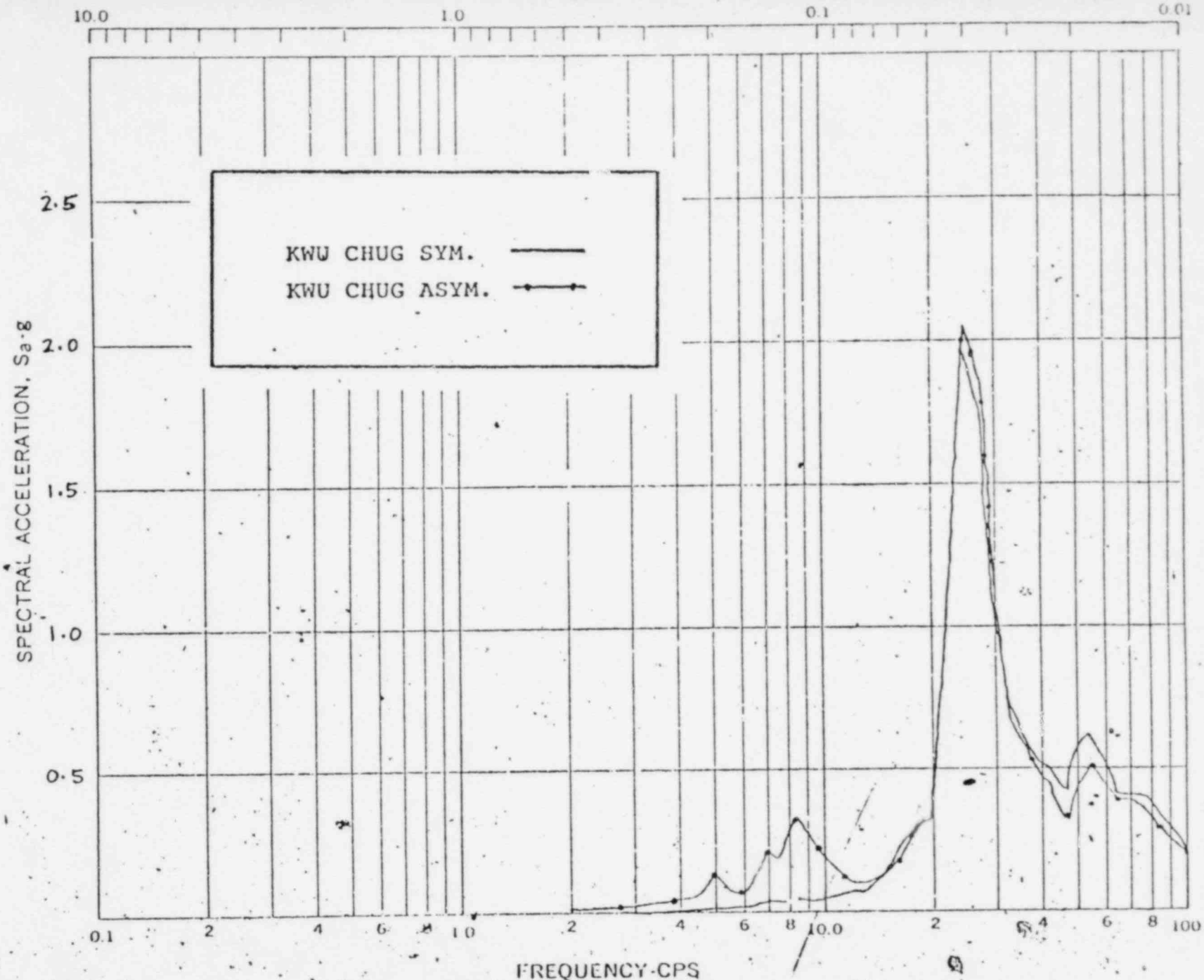

Acceleration Spectra for CONTAINMENT SHELL

Load Case: Surryshenng1 KWU CHUG SYM. VS ASYM.

Node 411, Direction X, Elev 778' - 9-3/4"

Damping 0.02

Figure 1-8

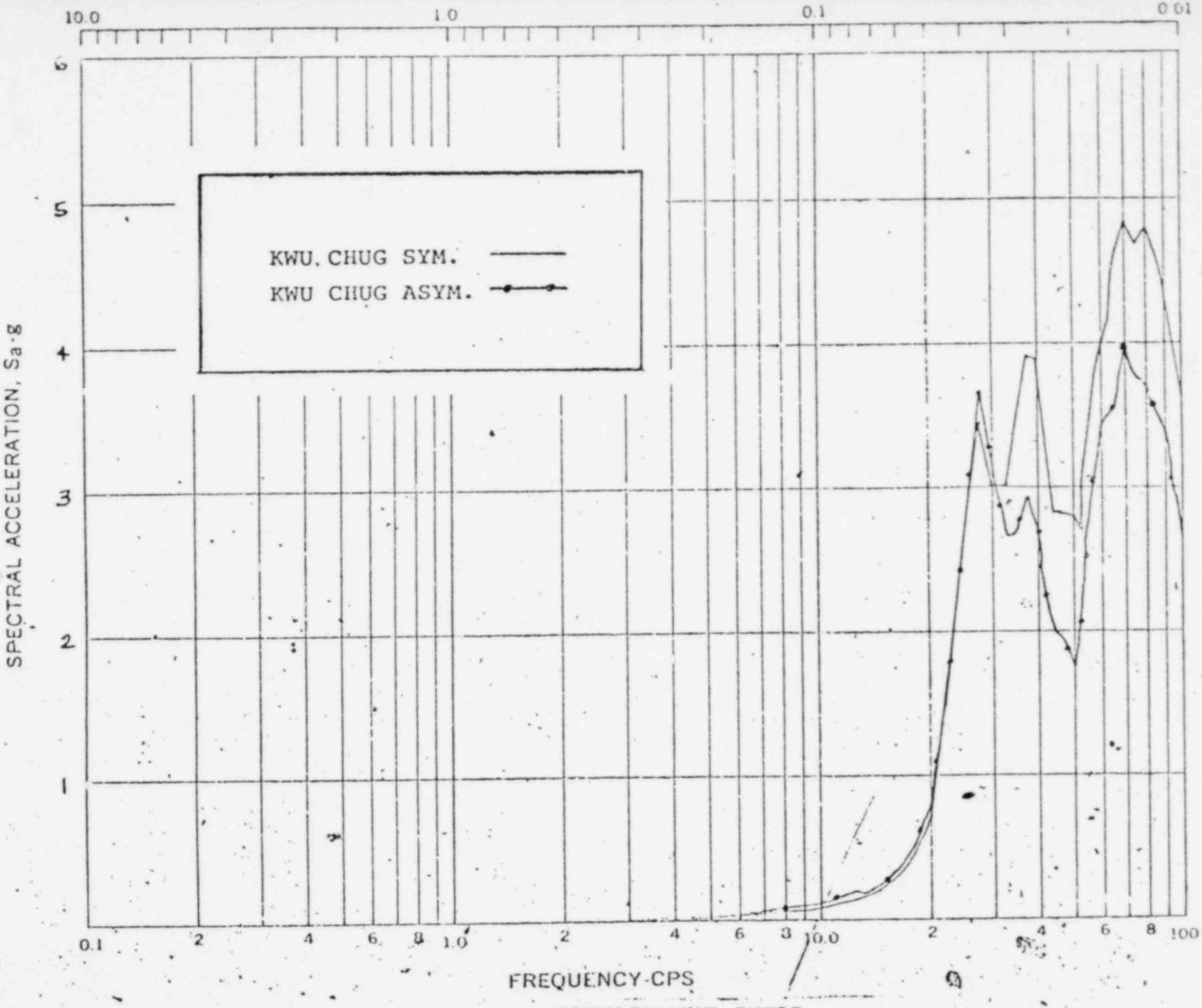

Acceleration Spectra for CONTAINMENT SHELL

Load Case: Susquehanna KWU CHUG SYM. VS ASYM.

Node 135, Direction Y, Elev 672'-0"

Damping: 0.02

Figure 1-9

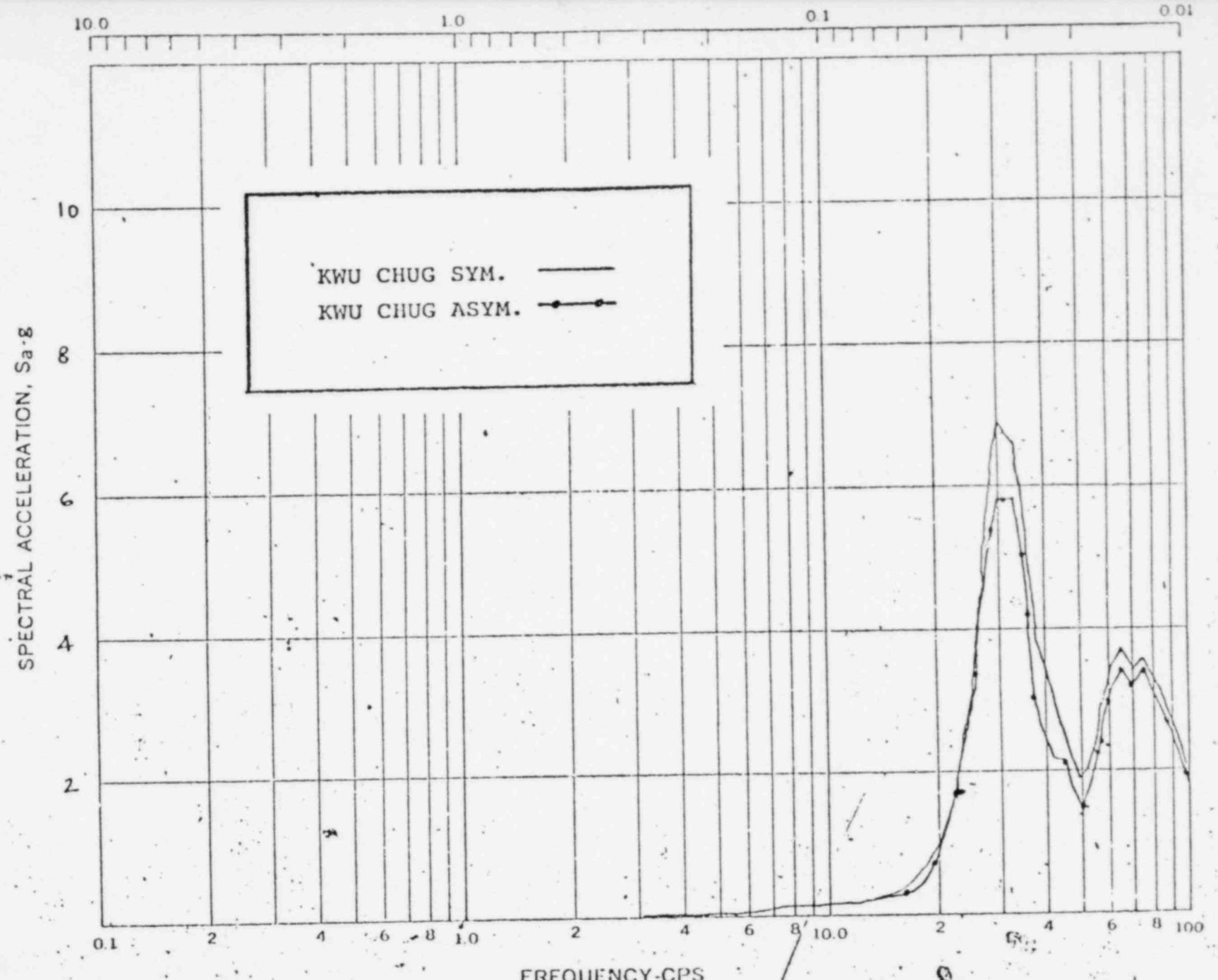

Acceleration Spectra for CONTAINMENT SHELL

Load Case: Susquehanna KWU CHUG SYM. VS ASYM.

Node 131, Direction X, Elev 672'-0"

Damping: 0.02

Figure 1-10

2.0 COMPARISON OF MINIMUM VARIANCE TRIALS USING THE SSES/GKM II-M SOURCES WITH THE JAERI DATA

2.1 INTRODUCTION

The SSES Chugging Loads Methodology specifies the use of the start time set (STS) that has the minimum variance in 1000 STSs drawn randomly from a 50 msec desynchronization time window. This minimum variance STS is then used for the application of all the SSES/GKM II-M Chugging Sources.

A given set of start times produces a unique pressure time history at the pool wall boundary, with signal attentuation (referred to as frequency holes) occurring at some frequencies and amplification at others, due to the vent-to-vent phasing implied by the selected set of start times. A concern was therefore raised that the use of a single STS in evaluating the SSES chugging loads might result in non-conservatisms in frequencies where signal attentuation or "frequency holes" occurred.

Although it is true that "frequency holes" will be produced with any one set of start times, the overall conservatism in the strengths of the SSES/GKM II-M Sources will still produce a conservative response of the SSES containment over the entire frequency range used in the plant structural evaluation. To demonstrate this, the SSES Chugging Loads calculation procedure was applied in the JAERI geometry and the results were compared against the bounding JAERI data. The following describes the comparison and presents the results obtained. The results confirm the conservatism in the SSES Chugging Load Definition.

2.2 COMPARISON PROCEDURE

First, one thousand STSs were drawn randomly from the 50 msec desynchronization time window. Note that each STS consists of seven start times--one for each of the seven vents in the JAERI geometry. The STS having the minimum variance was then identified. This procedure was repeated 20 times and 20 such minimum variances STSs were obtained.

Using each minimum variance STS, the SSES/GKM II-M chug sources were applied one at a time in an acoustic model of the JAERI test facility. Spatially averaged pressure time histories (one for each source) were then generated at the 1.8 meter and 3.6 meter elevations. The power spectral densities (PSD) were then obtained for these pressure time histories. From these, PSD envelopes over the SSES/GKM II-M sources were constructed at the 1.8 meter and 3.6 meter elevations. Similarly, PRS envelopes were obtained at the 1.8 meter elevation. This procedure was performed using each of the 20 minimum variance STSs. Thus, at each of the two elevations, 20 PSD envelopes resulted--one for each of the 20 minimum variance STSs, and 20 PRS envelopes were obtained at the 1.8 meter elevation.

Finally, minimum PSD envelopes for the 20 minimum variance STS were constructed at the 1.8 meter and 3.6 meter elevations; minimum PRS envelope was constructed at the 1.8 meter elevation. These minimum PSD and PRS envelopes were then compared with the corresponding maximum envelopes of the eight largest chugs for JAERI test 0002. Note that the PRSs for the JAERI data were obtained by digitizing the JAERI pressure time histories to produce the respective PRSs. The comparison and conclusions are presented in the next section.

Before proceeding to discuss results, several important points require further clarification. First, the SSES/GKM II-M Sources used in the JAERI acoustic model to calculate the JAERI pool wall pressure time histories used the same sonic speed as that given in the SSES Chugging load definition report. That is, the sonic speeds derived for the GKM II-M test facility were used with each of the SSES/GKM II-M sources. The sonic speeds for the SSES/GKM II-M ranges between 661m/sec and 449 m/sec.

The sonic speeds in flexible wall facilities are related to the equivalent rigid wall sonic speeds by the following relation:

$$C = C_o(1+\rho C_o^2 \delta)^{-\frac{1}{2}}$$

where ρ is the water density, C is the flexible wall sonic speed, C_o is the rigid wall sonic speed and δ is volume distensibility*. Figure 2-1 shows the relationships between the rigid wall sonic speeds and flexible wall sonic speeds for GKM II-M and JAERI facilities.

Ideally, the GKM II-M "rigid wall" sonic speeds would be obtained first by using the above relation. The rigid wall sonic speeds would then be corrected to obtain the equivalent flexible wall sonic speeds for JAERI. These corrected sonic speeds would then be used with the corresponding sources in the JAERI acoustic model for predicting the JAERI wall pressures. However, this procedure was not used because the differences between the GKM II -M flexible wall sonic speeds and the corresponding JAERI flexible wall sonic speeds is less than 7% over the range of sonic speeds (661 m/sec to 449 m/sec) for the SSES/GKM II-M sources.** This small difference did not warrant the added computational complexity and hence the GKM II-M sonic speeds were used in the JAERI wall pressure computations.

---

* $\delta = 139.90 \times 10^{-12}$ m/n^2 for GKM II-M facility.

$\delta = 497.38 \times 10^{-12}$ m/n^2 for JAERI facility.

** This is because most of the "flexibility" comes from the air in the pool rather than from the structural flexibility.

The second point that needs to be clarified is with respect to the damping values used in the calculation of the PRSs. The PRSs were calculated using 4% and 7% damping. These are the damping values described in USAEC Reg. Guide 1.61 for reinforced concrete containments.

The final point is regarding the amplitude factors used with the sources. The SSES Chugging Loads methodology calls for multiplying the SSES/GKM II-M sources by an amplitude factor to achieve an exceedance probability of 10^{-5}. For the 87 vent SSES containment geometry, an amplitude factor of 1.3 is derived.

Since the objective of the comparisons presented here is to compare the results of applying the SSES Chugging Loads Methodology in JAERI with the actual JAERI data, one must compute the amplitude factor appropriate for the seven vent JAERI geometry. The amplitude factor for the JAERI seven vent geometry is 1.95 to obtain an exceedance probability of 10^{-5} used for the SSES plant evaluations. The comparisons presented in the next subsection are made using the amplitude factor of 1.3 corresponding to that used for the SSES Chugging Loads evaluations as well as the amplitude factor of 1.95 which is the correct one for application of the SSES Chugging Loads Methodology in the JAERI facility.

2.3 RESULTS AND DISCUSSION

As described in the previous Subsection, two types of comparisons were performed--one on a PSD basis and one on a PRS basis. The PSD comparisons are presented in Subsection 2.3.1 followed by the PRS comparisons in Subsection 2.3.2.

2.3.1 PSD Comparisons

Figure 2-2 shows the comparison of the minimum envelope of 20 minimum variance STSs with the JAERI data at the 1.8 meter elevation. The amplitude factor used here was that for the SSES containment and equal to 1.3. From this figure it is seen that the minimum envelope of the 20 minimum variance STSs bounds the JAERI data by a substantial margin at frequencies below about 40 Hz. Above 40 Hz, the signal levels are quite small and so from this linear plot it is difficult to make many comparisons. Therefore, the same data plotted on log scale are shown in Figure 2-3. From this figure it is seen that the minimum envelope drops below the maximum JAERI data envelope by a small amount in the frequency range between 40 and 80 Hz.

Figure 2-4 shows the comparison of the minimum envelope of 20 minimum variance STSs with the maximum JAERI data envelope at the 3.6 meter elevation. From this linear plot, it is again seen that the minimum envelope of the 20 minimum variance STSs bounds the JAERI data envelope by substantial margins and both the JAERI data envelope as well as the 20 minimum variance STSs en-

velope drop to very low levels beyond 30 Hz. Figure 2-5 shows the same data plotted on a log scale, and it is seen that in the frequency range between 40 and 60 Hz, the JAERI data envelope "pokes through" the minimum envelope by small amounts.

As mentioned earlier in Section 2.2, the appropriate amplitude factor for the seven vent JAERI geometry is 1.95. Comparisons are now made using the 1.95 amplitude factor. Figure 2-6 shows the comparison of the minimum envelope of 20 minimum variance STSs with the maximum JAERI data envelope at the 1.8 meter elevation. It is seen that with this amplitude factor of 1.95, the minimum variance envelope bounds the JAERI data by substantial margins everywhere except for some small "poke throughs" in the frequency range between 45 and 80 Hz. Figure 2-7 shows a similar comparison at the 3.6 meter elevation and at this elevation, the minimum envelope of the 20 minimum variance STSs bounds the JAERI data at all frequencies.

From the comparisons presented above, the following conclusions can be drawn:

1. Using an amplitude factor of 1.3 (the SSES value), the minimum envelope of 20 minimum variance trials bounds the maximum envelope of JAERI data except for small "poke throughs" between approximately 40 and 80 Hz.

2. Using an amplitude factor of 1.95 which is the correct factor for the seven vent JAERI geometry, the minimum envelope of the 20 minimum variance trials bounds the maximum envelope of JAERI data everywhere at the 3.6 meter elevation and there are very small "poke throughs" between 40 and 80 Hz at the 1.8 meter elevation.

2.3.2 Pressure Response Spectra Comparisons

Comparisons on PRS basis are more appropriate than PSD comparisons in evaluating the effect of a given pressure time history on a multi-modal structure such as the SSES containment. This is because the response of the multi-modal structure at a given modal frequency is the sum of the resonant response to forcing function amplitude at the modal resonant frequency plus the static or forced response due to forcing function amplitudes at other frequencies. A PSD only shows the component of the forcing function at a given frequency and therefore, does not provide insight into the static or forced response of the structure. A PRS on the other hand takes into account both the resonant and the static or forced response and hence provides a more accurate picture of the response of a multi-modal system.

The comparison of the minimum PRS envelope for the 20 minimum variance STSs with the maximum PRS envelope of the JAERI data at the 1.8 meter elevation is shown in figure 2-8. For the PRSs shown in this figure, the SSES amplitude factor of 1.3 was used with a damping value 4%. It is clear from this figure that the minimum envelope of the 20 minimum variance STSs bounds the maximum PRS envelope of the JAERI data throughout the frequency range between 0-100 Hz. Figure 2-9 shows the PRS comparisons for an amplitude of 1.95, and a 4% damping. Again this figure shows that the minimum envelope of the 20 minimum variance trials bounds the maximum JAERI data envelope by significant margins across the entire frequency range.

Finally, Figures 2-10 and 2-11 show the PRS envelope comparisons for the 7% damping case with amplitude factors of 1.3 and 1.95 respectively. From these figures it is again seen that the minimum PRS envelope of the 20 minimum variance STSs bounds the maximum JAERI data PRS envelope by a substantial margin throughout the frequency range.

From the comparisons presented above, it can be concluded that due to the large conservatisms in the strength of the SSES/GKM II-M Sources, the response produced by the minimum variance STSs will produce conservative plant responses in spite of the "frequency holes" created by a particular STS selection. Therefore, the SSES/GKM II-M Chugging Loads Methodology is adequate.

3.0 REFERENCES

1. Letter from Roger J. Mateson, Office of Nuclear Reactor Regulations, to Dr. H. Chau, Chairman of the Mark II Owners Group, dated February 25, 1982.

2. Letter from G. D. Bouchey to A. Schwencer, Desynchronization Methodology in the Chugging Load Specification, dated March 15, 1982, Letter No. G02-82-324.

3. Letter from G. D. Bouchey to A. Schwencer, Comparison of Structural Response to Symmetric and Asymmetric Chugging and Seismic Loads, dated April 5, 1982, Letter No. G02-82-362.

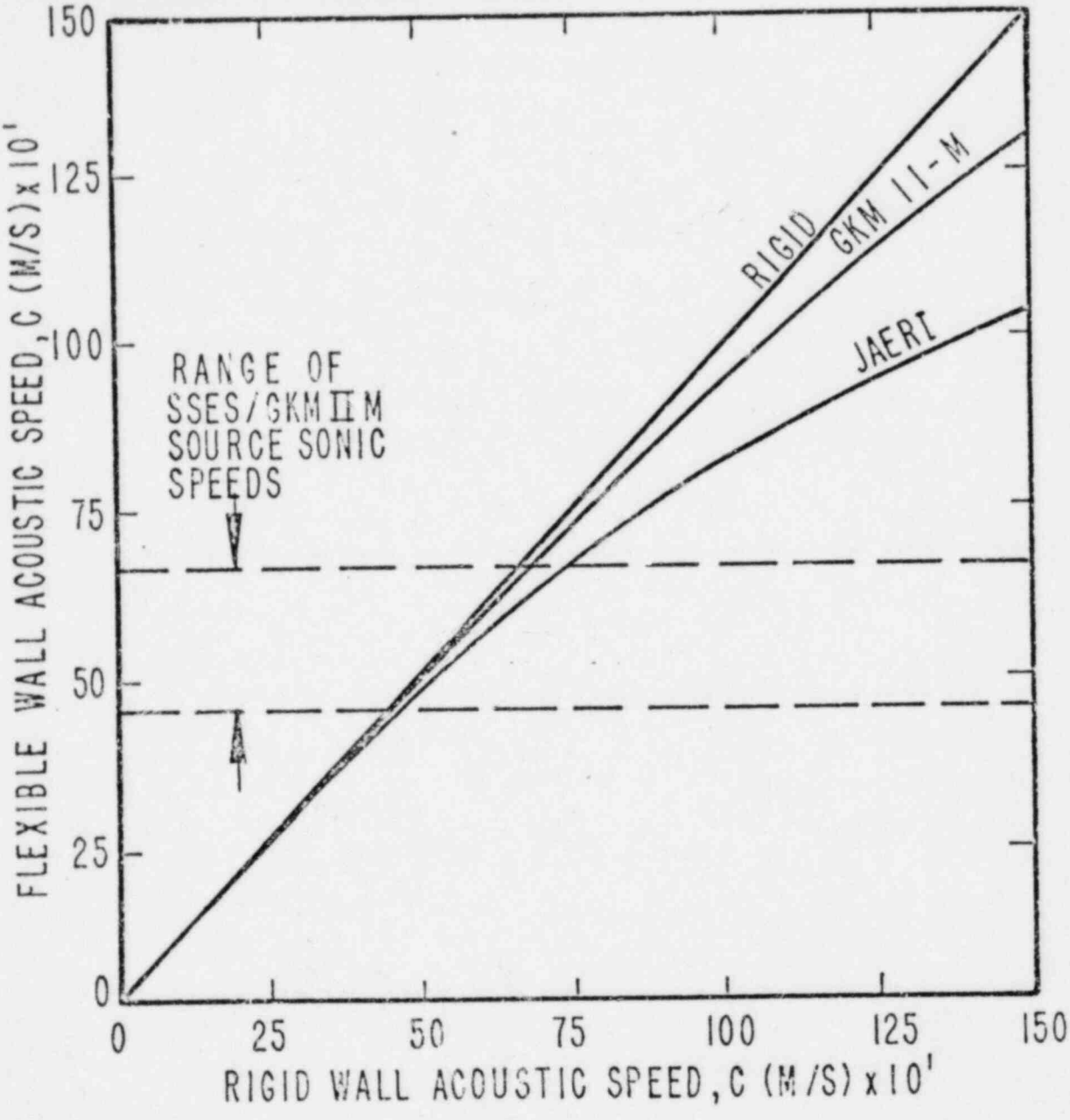

Figure 2-1. COMPARISON OF FLEXIBLE WALL SONIC SPEEDS IN GKMIIM AND JAERI TEST FACILITIES.

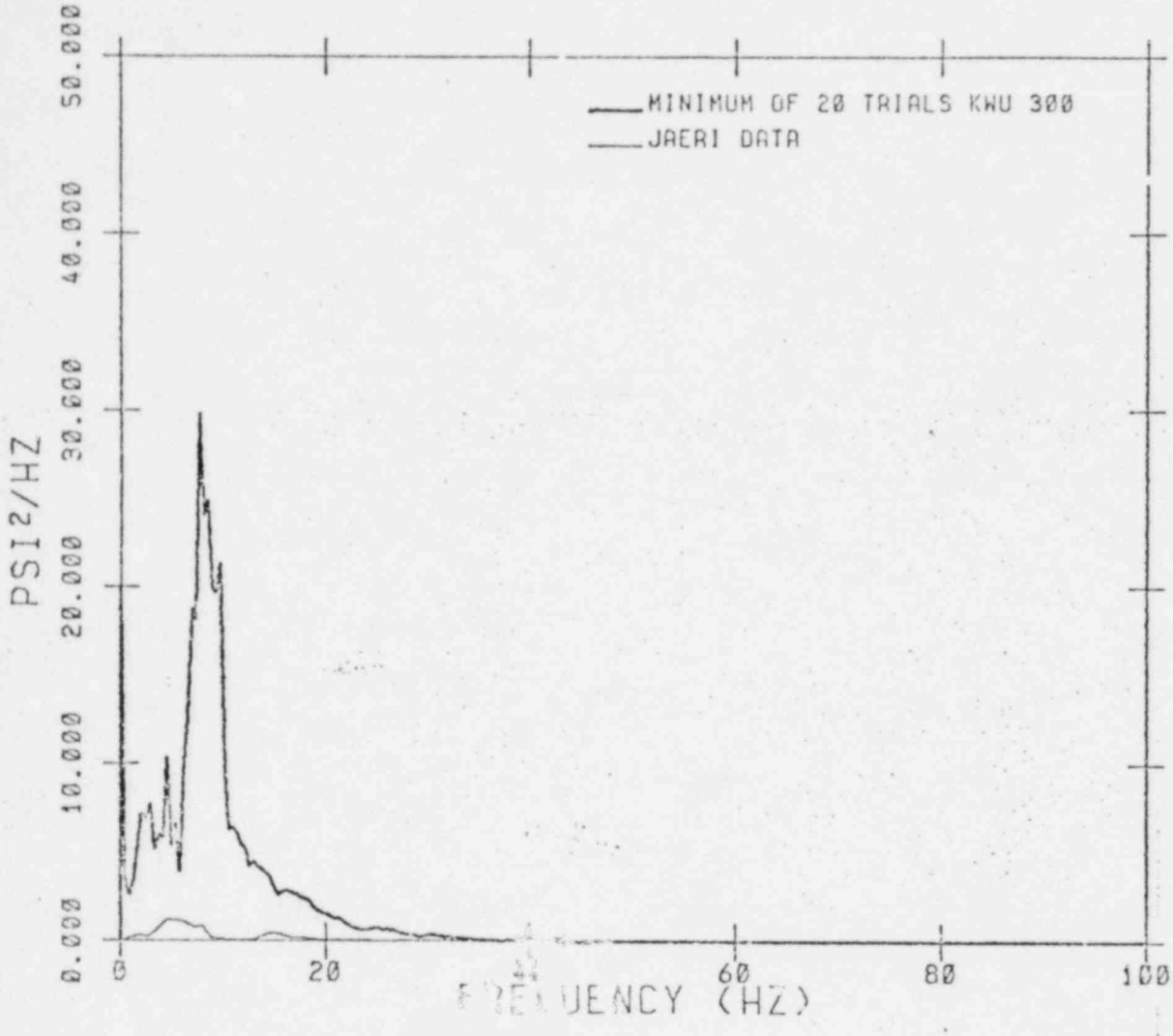

Figure 2-2 COMPARISON OF THE MINIMUM PSD ENVELOPE OF 20 MIN. VAR. STS TRIALS WITH MAXIMUM PSD ENVELOPE OF JAERI DATA AT 1.8M ELEVATION--AMPLITUDE FACTOR 1.3.

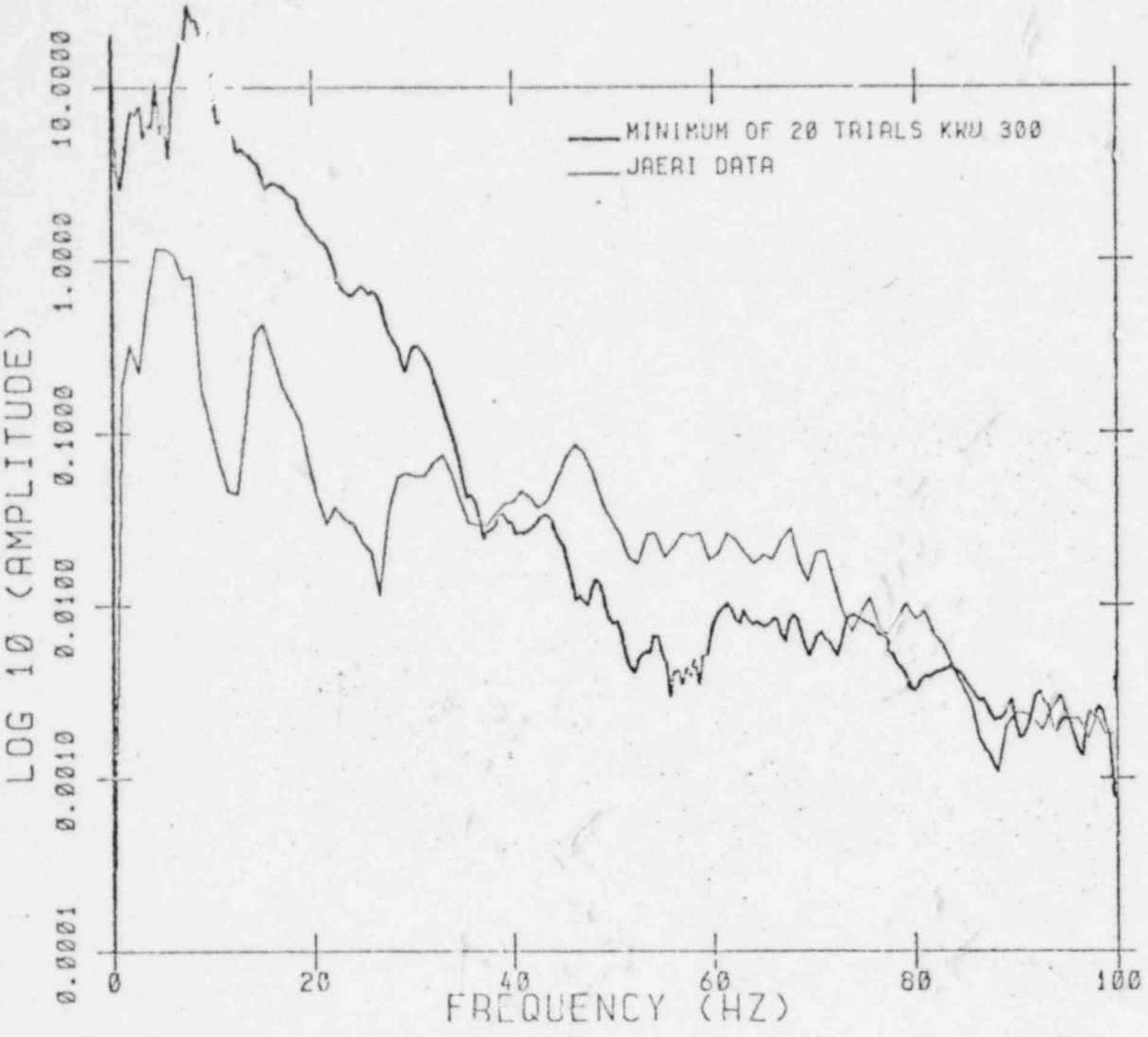

Figure 2-3 COMPARISON OF THE MINIMUM PSD ENVELOPE OF 20 MIN. VAR. STS TRIALS WITH MAXIMUM PSD ENVELOPE OF JAERI DATA AT 1.8M ELEVATION--AMPLITUDE FACTOR 1.3.

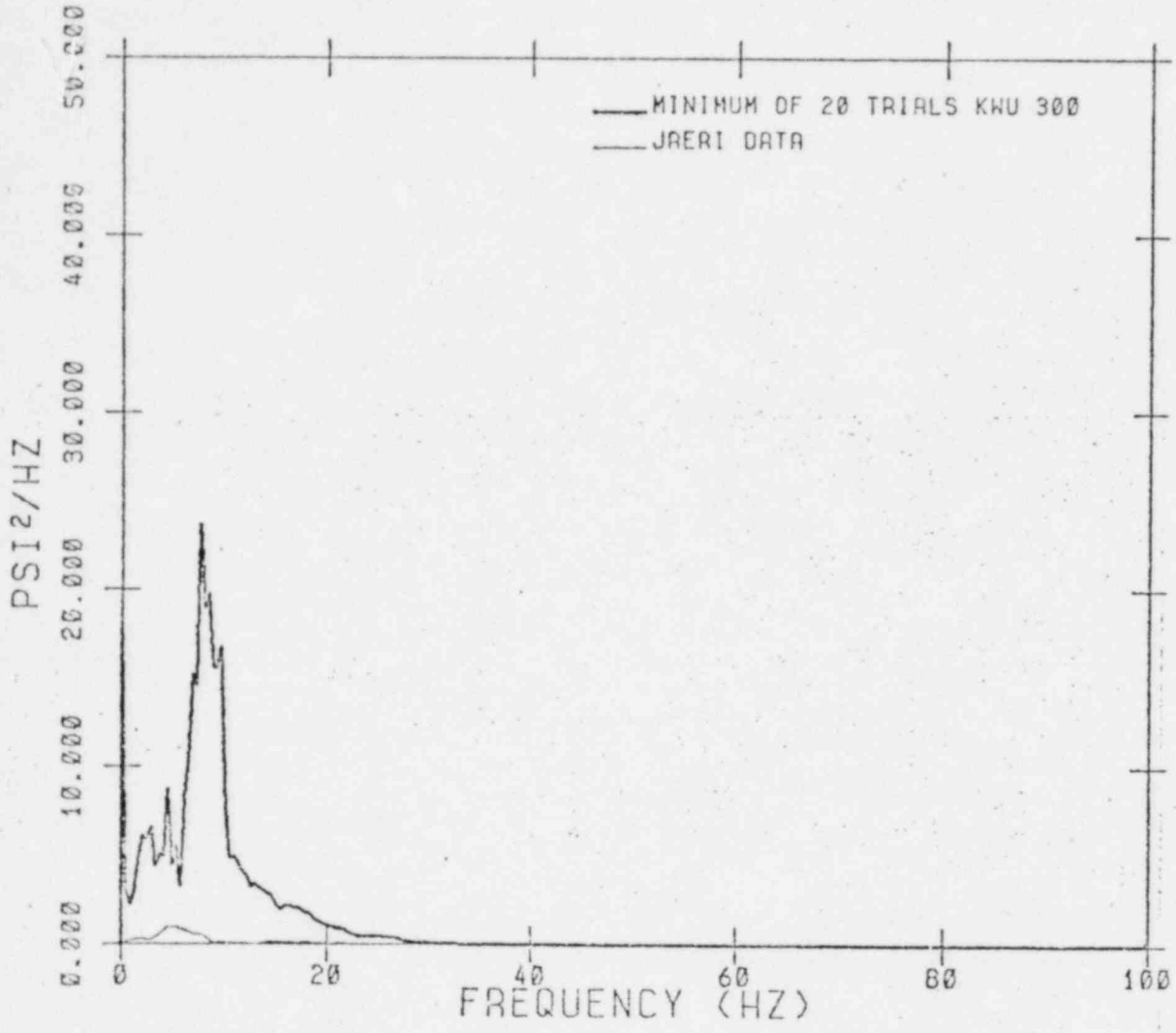

Figure 2-4. COMPARISON OF THE MINIMUM PSD ENVELOPE OF 20 MIN. VAR. STS TRIALS WITH MAXIMUM PSD ENVELOPE OF JAERI DATA AT 3.6 M ELEVATION--AMPLITUDE FACTOR 1.3.

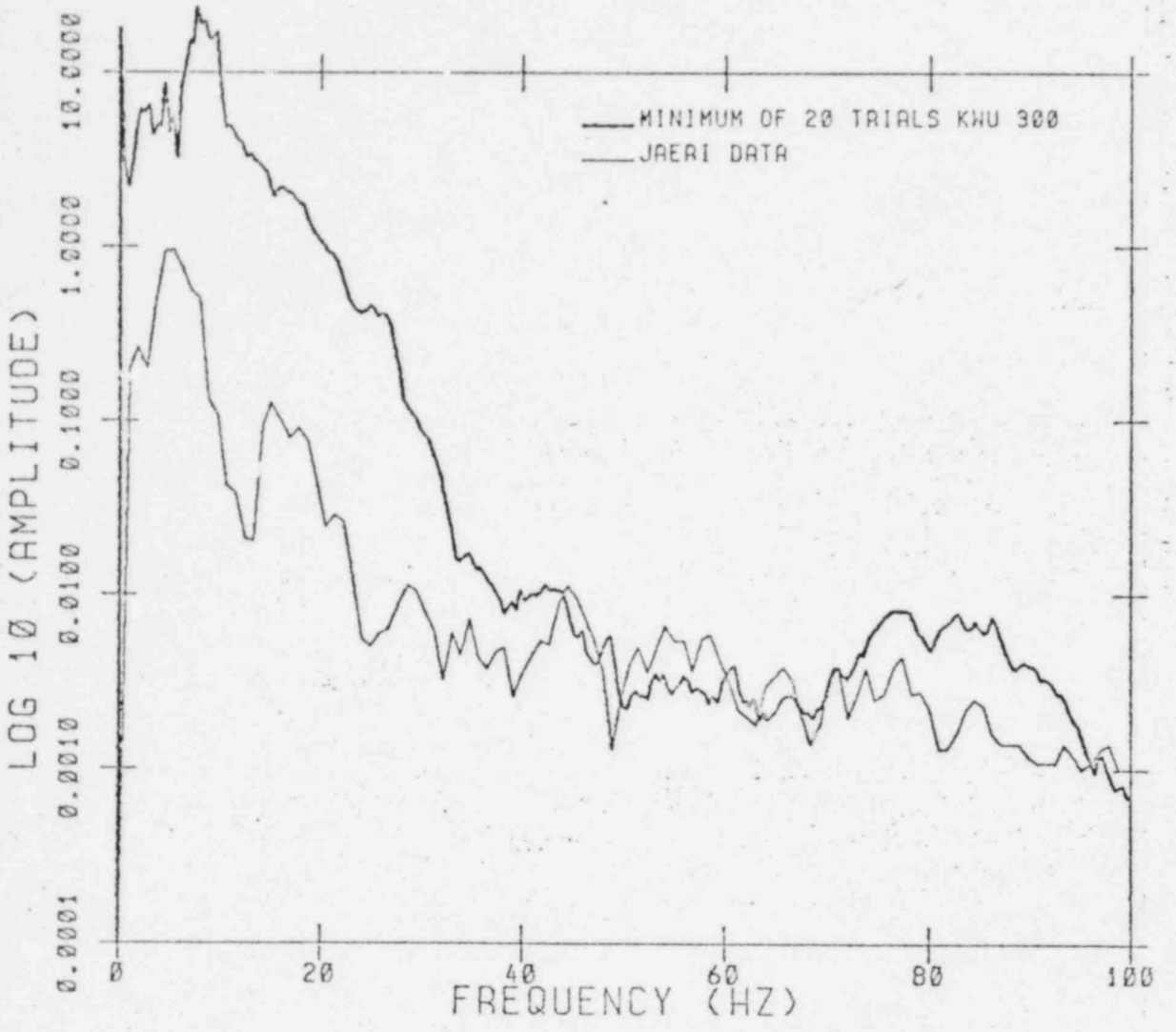

Figure 2-5. COMPARISON OF THE MINIMUM PSD ENVELOPE OF 20 MIN. VAR. STS TRIALS WITH MAXIMUM PSD ENVELOPE OF JAERI DATA AT 3.6 M ELEVATION--AMPLITUDE FACTOR 1.3.

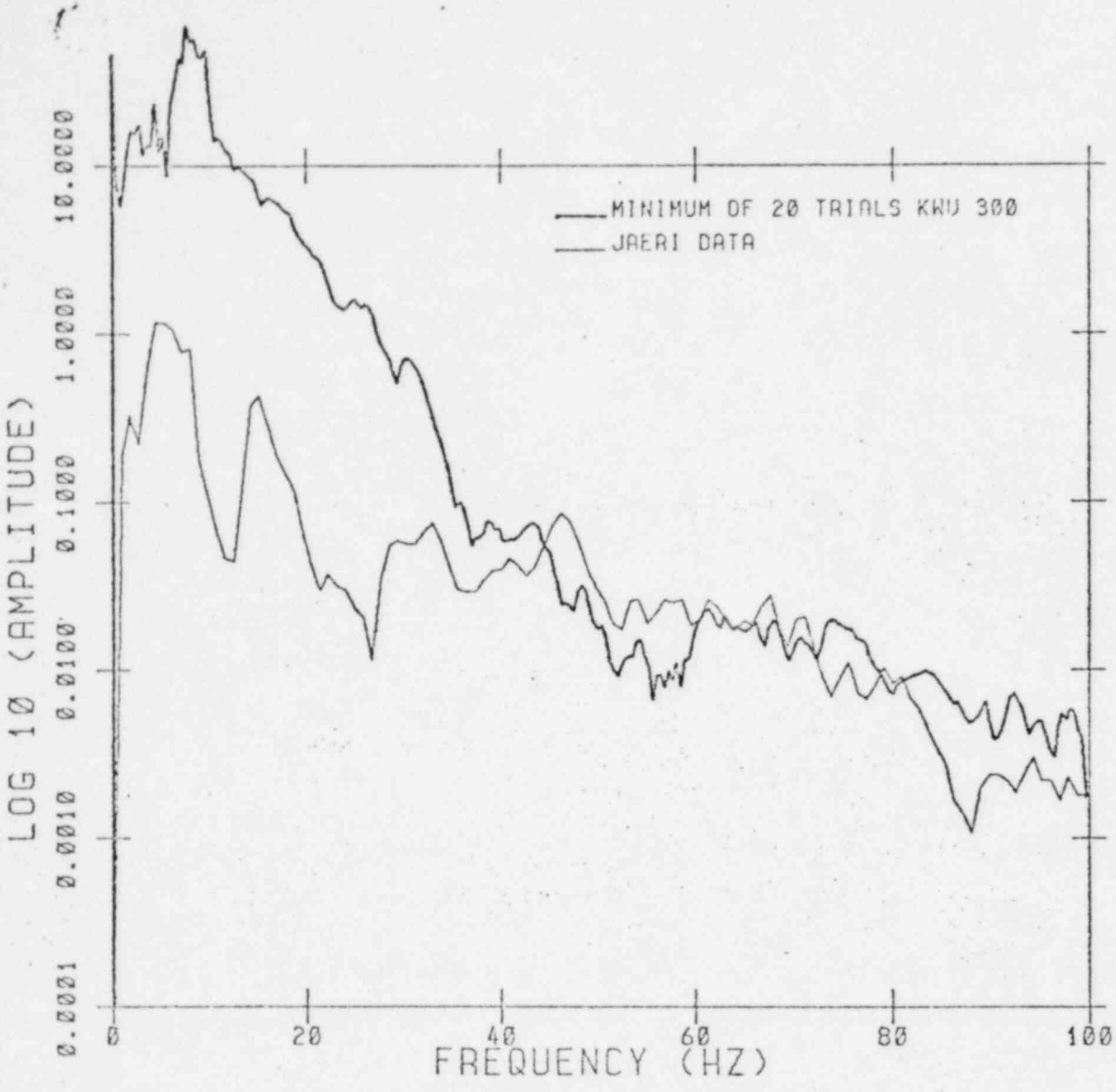

Figure 2-6. COMPARISON OF THE MINIMUM PSD ENVELOPE OF 20 MIN. VAR. STS TRIALS WITH MAXIMUM PSD ENVELOPE OF JAERI DATA AT 1.8 M ELEVATION--AMPLITUDE FACTOR 1.95.

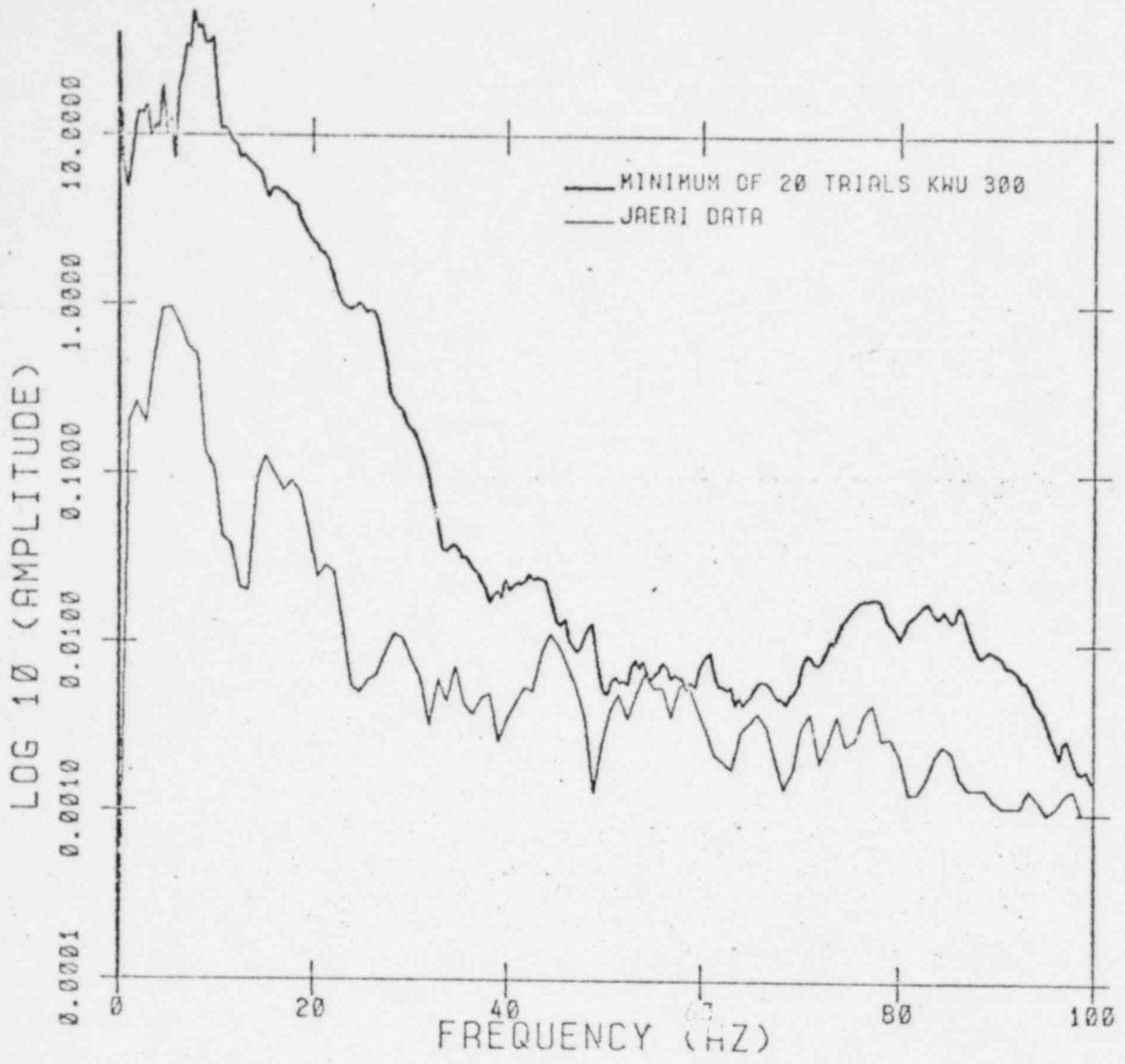

Figure 2-7. COMPARISON OF THE MINIMUM PSD ENVELOPE OF 20 MIN. VAR. STS TRIALS WITH MAXIMUM PSD ENVELOPE OF JAERI DATA AT 3.6 M ELEVATION -- AMPLITUDE FACTOR 1.95.

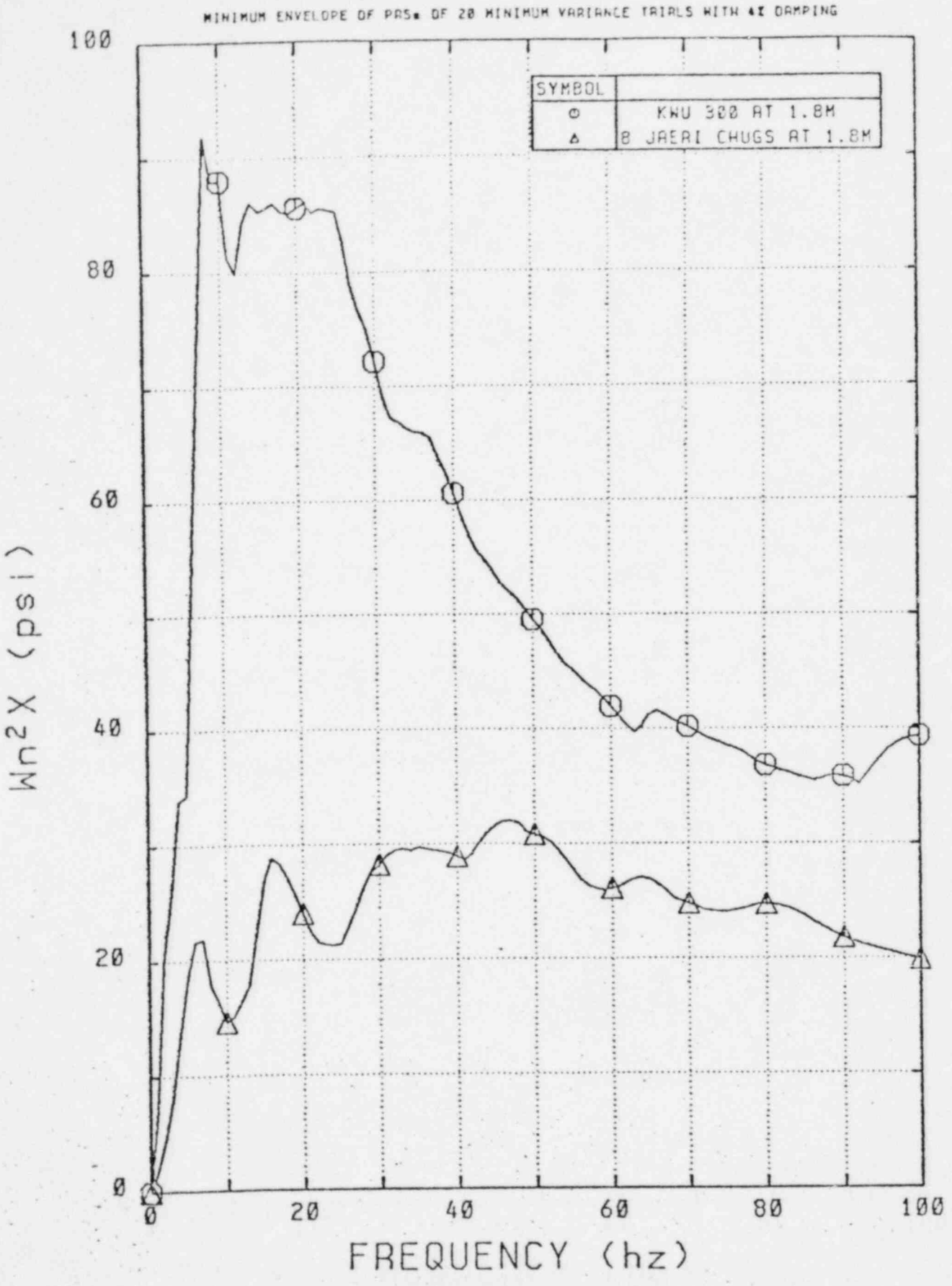

Figure 2-8. COMPARISON OF THE MINIMUM PRS ENVELOPE FOR THE 20 MIN. VAR. STS TRIALS WITH THE MAXIMUM PRS ENVELOPE OF THE JAERI DATA--AMPLITUDE FACTOR 1.3, DAMPING 4%.

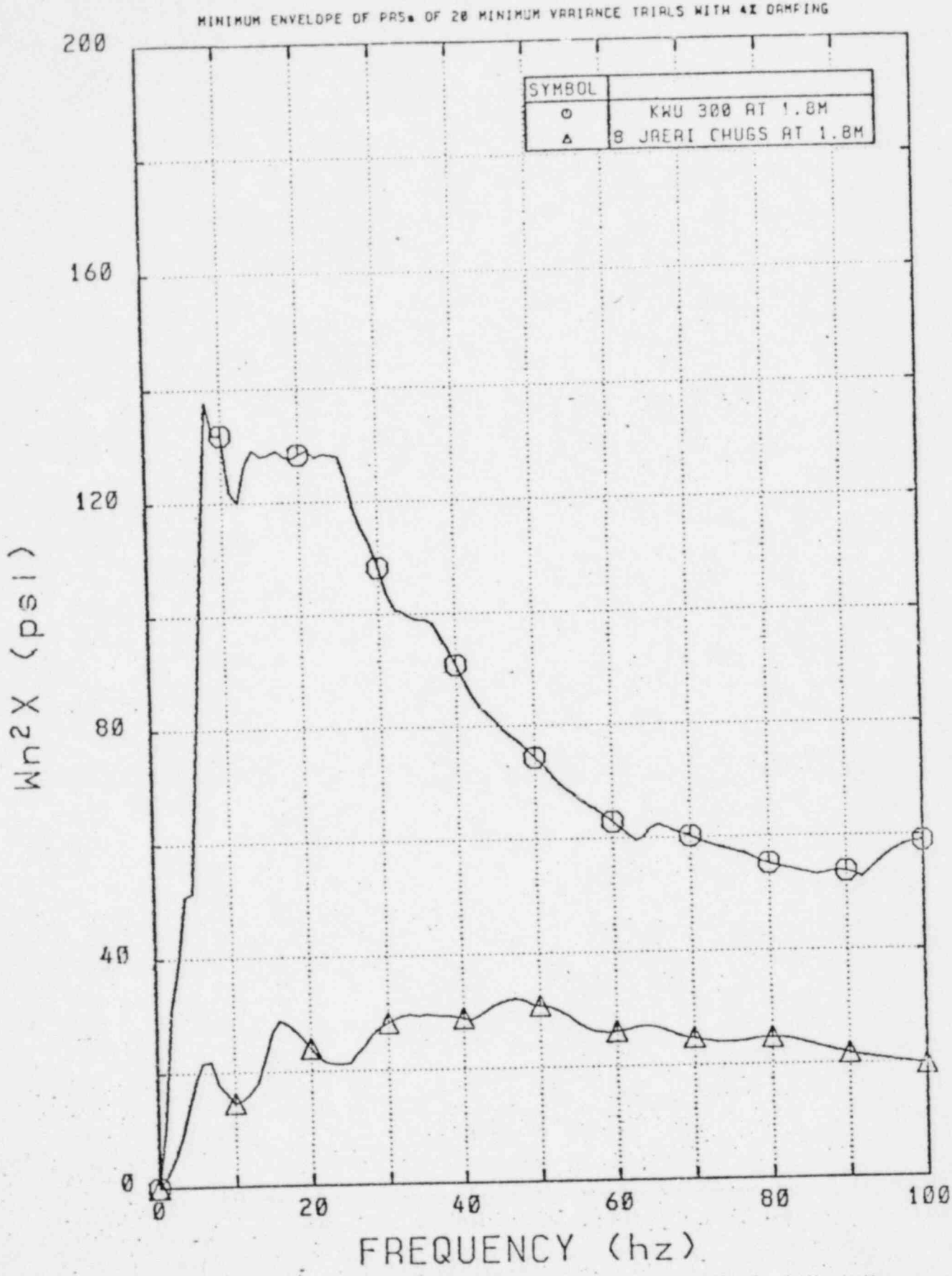

Figure 2-9 COMPARISON OF THE MINIMUM PRS ENVELOPE FOR THE 20 MIN. VAR. STS TRIALS WITH THE MAXIMUM PRS ENVELOPE OF THE JAERI DATA--AMPLITUDE FACTOR 1.95 DAMPING 4%.

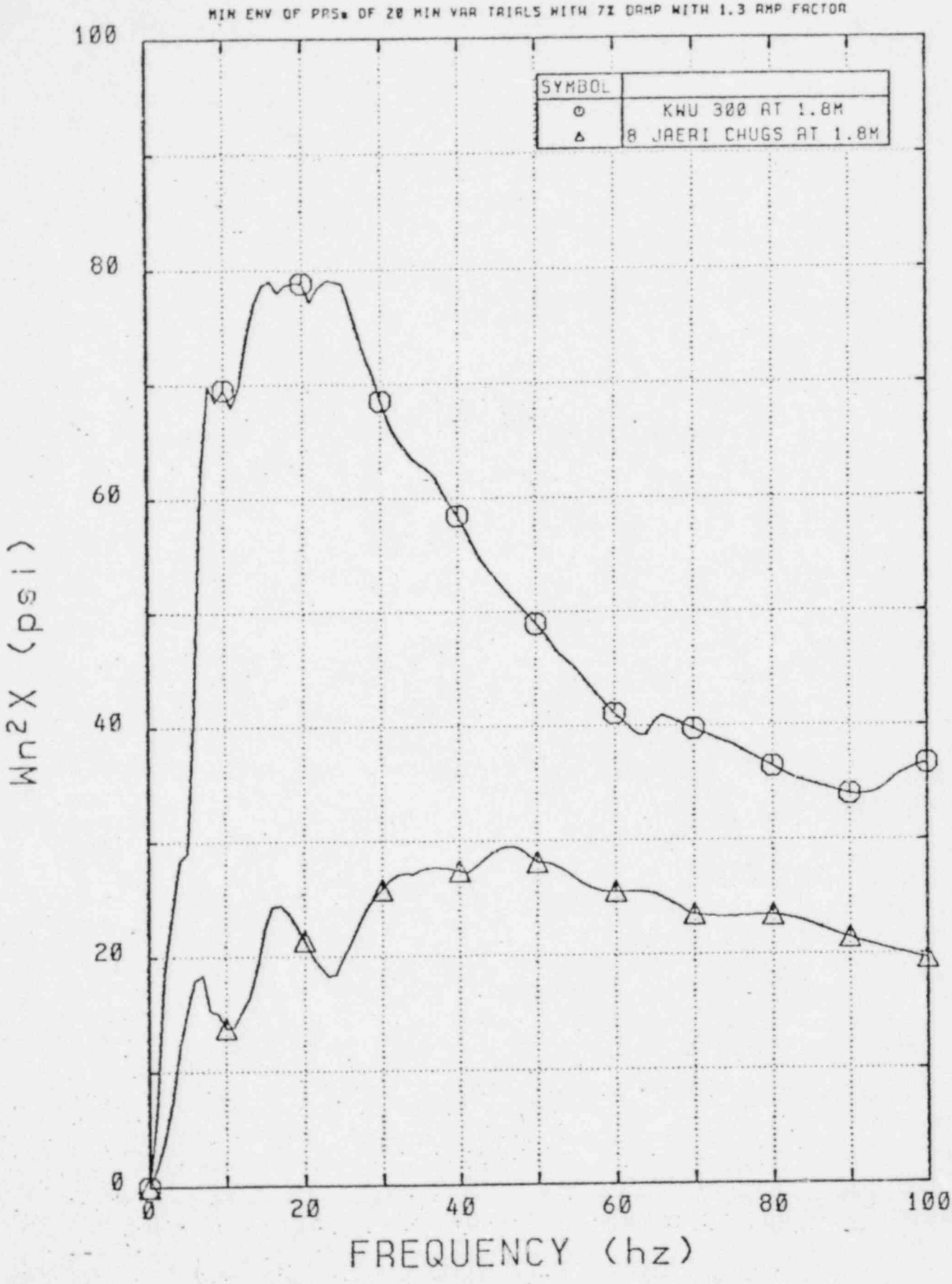

Figure 2-10. COMPARISON OF THE MINIMUM PRS ENVELOPE FOR THE 20 MIN. VAR. STS TRIALS WITH THE MAXIMUM PRS ENVELOPE OF THE JAERI DATA--AMPLITUDE FACTOR 1.3 DAMPING 7%.

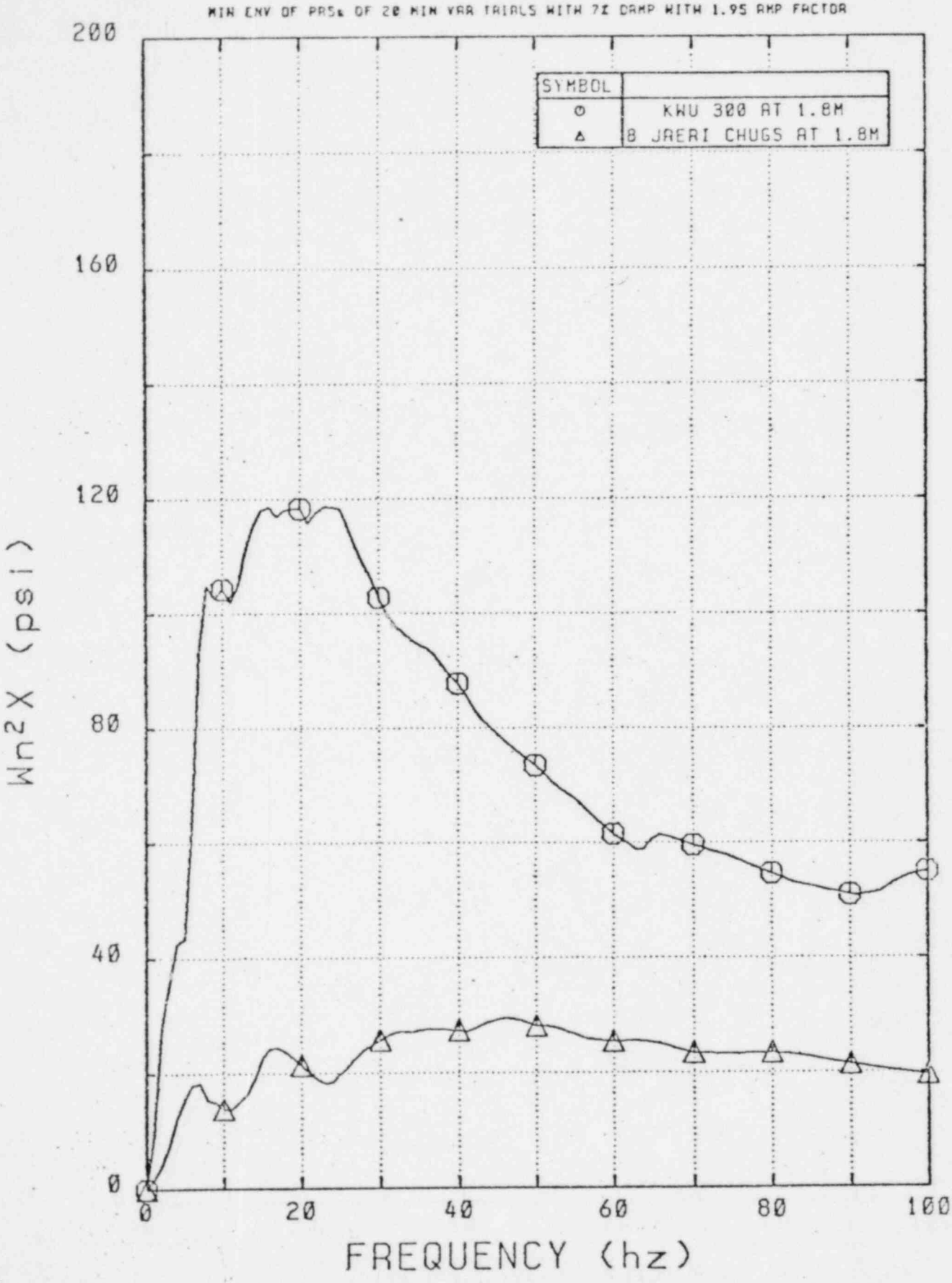

Figure 2-11. COMPARISON OF THE MINIMUM PRS ENVELOPE FOR THE 20 MIN. VAR. STS TRIALS WITH THE MAXIMUM PRS ENVELOPE OF THE JAERI DATA--AMPLITUDE FACTOR 1.95, DAMPING 7%.